Energy 302 (2024) 131762

Contents lists available at ScienceDirect

Energy

journal homepage: www.elsevier.com/locate/energy

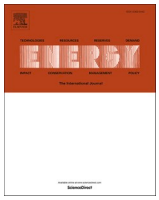

Selective H_2 production from plastic waste through pyrolysis and in-line oxidative steam reforming

Mayra Alejandra Suarez [a], Katarzyna Januszewicz [b], Maria Cortazar [a], Gartzen Lopez [a,c,*], Laura Santamaria [a], Martin Olazar [a], Maite Artetxe [a], Maider Amutio [a]

[a] Department of Chemical Engineering, University of the Basque Country UPV/EHU, P.O. Box 644, E48080, Bilbao, Spain
[b] Department of Energy Conversion and Storage, Chemical Faculty, Gdańsk University of Technology, Narutowicza 11/12, 80-233, Gdańsk, Poland
[c] IKERBASQUE, Basque Foundation for Science, Bilbao, Spain

ARTICLE INFO

Handling editor: Krzysztof (K.J.) Ptasinski

Keywords:
Hydrogen
Pyrolysis
Oxidative-reforming
Plastic waste
Autothermal

ABSTRACT

This study deals with the proposal of pyrolysis and in-line oxidative steam reforming (P-OSR) for plastic waste valorization and assesses the potential of this strategy for the selective production of H_2. Overall, the study aims at progressing towards the fine-tuning of the pyrolysis-reforming technology by co-feeding O_2. Thus, a multi-point O_2 injection system has been developed to ensure a suitable O_2 distribution in the reforming reactor and avoid the formation of hot spots, as they may cause catalyst deactivation by metal sintering. Moreover, as O_2 is directly supplied into the catalytic bed, pre-combustion of the volatile stream before contacting the catalyst is avoided and in-situ coke combustion is promoted. The P-OSR of HDPE was carried out in a two-step reaction system, which combines CSBR (conical spouted bed reactor) and FBR (fluidized bed reactor) technologies. The experiments were conducted in continuous mode and the influence of the main process conditions at zero time on stream was analyzed. Thus, the effect of reforming temperature was studied in the 550–750 °C range, that of the space time from 3.12 to 15.62 g_{cat} min g_{HDPE}^{-1}, steam to plastic (S/P) ratio between 2 and 5 and equivalence ratio (ER) from 0 to 0.3. Under the optimum conditions (700 °C, S/P of 3, 12.5 g_{cat} min g_{HDPE}^{-1} and ER of 0.2), a H_2 production of 25.0 wt% was obtained, which is only 28.6 % lower than that obtained in the conventional pyrolysis-steam reforming (P-SR) process. The results obtained confirm the potential of continuous P-OSR process for the selective production of H_2.

1. Introduction

Plastics are a family of materials with great versatility and excellent properties, such as lightness, insulation or conductivity, transparency or opacity, corrosion and chemical resistance, and durability or biodegradability, which make them unique materials. Therefore, nowadays plastics are the most used materials for a huge number of products coming from different sectors. In 2021, after the stagnation due to Covid-19 pandemic in 2020, the global plastic production increased to 390.7 million tons (Mt). The world plastic manufacturing is led by far by China, reaching almost one third of the total production, followed by North America (18 %) and Europe (15 %). In terms of applicability, they are mainly used in packaging (44 %), building and construction (18 %), and automotive sector (8 %). However, once they have been used, plastic products turned into waste, which must be properly managed [1].

A suitable plastic waste management is crucial to progress towards a greater sustainability, and therefore to a circular economy [2–4]. Although the treatment of plastic wastes has considerably evolved in the last 15 years, an inadequate collection and disposal have led to a relentless growing of plastic pollution, harming the environment and biodiversity [5,6]. In 2020, 29.5 million tons of post-consumer plastic wastes were collected in Europe, with 42 % being recovered for energy (incinerated), 35 % recycled and 23 % landfilled [1]. Currently, the mixed plastic wastes, which are potentially contaminated, are disposed in landfills or incinerated, since mechanical recycling is not a viable solution. In these cases, chemical recycling becomes a feasible solution [7–10].

Chemical recycling refers to a wide range of emerging technologies and processes aimed at turning plastic wastes into value-added products, and therefore, boosting circularity. Chemical recycling does not replace mechanical recycling, but is a complimentary one that may promote the

* Corresponding author. Department of Chemical Engineering, University of the Basque Country UPV/EHU, P.O. Box 644, E48080, Bilbao, Spain.
E-mail address: gartzen.lopez@ehu.es (G. Lopez).

https://doi.org/10.1016/j.energy.2024.131762
Received 14 December 2023; Received in revised form 27 March 2024; Accepted 22 May 2024
Available online 24 May 2024

development of new routes for plastic waste management. However, there are still crucial challenges ahead that must be overcome. Briefly, chemical recycling breaks down the plastic's polymeric chains into small molecules including monomers to produce fuels and chemicals [11–13]. Amongst the chemical recycling routes for plastics upgrading, thermochemical processes arise as promising ones, as they have already been developed to pilot and demonstration scale [14–19].

Both pyrolysis and gasification processes have a great tolerance to tackle hard-to-treat waste streams [14,20–24]. Whereas pyrolysis is carried out at mild temperatures under inert atmosphere and produces a wide product distribution, gasification is conducted at higher temperatures (>700 °C) using a gasifying agent (steam, air, CO_2 or mixtures) and is more selective [25,26]. On the one hand, depending on the operating conditions used in the pyrolysis process, i.e., residence time, temperature and heating rate, it may be driven to obtain high value added products, such as fuels (diesel and gasoline fractions) or chemicals (olefins, BTX and so on) [27]. Reactor configuration (screw kiln, fluidized bed reactor, spouted bed reactor) and catalysts (FCC, HZSM-5, Hβ zeolite, etc.) have a great influence on product distribution [28,29]. On the other hand, the gasification of waste plastics pursues the production of a tar-free syngas, which can be used as a fuel for heating and power generation or as a raw material for the synthesis of other fuels and chemicals, such as methanol, dimethyl ether and ammonia [30–33]. However, early industry investment in plastic-to-plastic chemical recycling is focusing on pyrolysis, driven by a combination of economics, feedstock tolerances and the relative availability of this technology, as it has been used in the actual fossil sources, namely pyrolysis oil displacing naphtha in steam crackers [7,34,35]. More recently, another process based on pyrolysis and in-line steam reforming (P-SR) strategy has been proposed for H_2 production from plastic wastes. Currently, most of the H_2 produced stems from fossil fuels, and therefore, the use of alternative raw materials, such as consumer society wastes, will help to reduce the dependency on non-renewable sources and alleviate the problems associated with global warming [36]. Thus, H_2 is mainly used for ammonia production (51 %), oil refining (31 %) or methanol synthesis (5 %). Besides, its potential as energy carrier makes it a suitable alternative for transformation into any form of energy for diverse end-use applications, namely transportation, variable renewable energy integration, or central heating [36]. This novel approach is made up of two steps, as are: a first step of pyrolysis carried out at low temperatures and a second one in which the plastic derived volatiles are transferred to the catalytic steam reforming process. Unlike gasification, this process may operate at lower temperatures, allows selecting the optimum conditions for each step and avoids the direct contact of plastic impurities with the reforming catalyst, thus preventing catalyst from fast deactivation [37,38].

It should be pointed out that the development of this novel strategy is still in an early stage. Although there are several studies in the literature dealing with this process in two lab scale fix bed reactors operating in batch mode [39–46], there are only few ones under continuous regime in bench scale plants [47–50]. In fact, the full-scale implementation of the P-SR process is highly conditioned by the type of technology and the development of specific catalysts. Thus, the high endothermicity of the steam reforming step as well as the severe coke formation, are the major challenges [36,51–54]. O_2 co-feeding may overcome the high energy requirements of the reforming step and contribute to the in-situ combustion of the coke, improving significantly the lifetime of the catalyst [55,56]. However, the presence of O_2 in the reforming reactor leads to the partial oxidation of the pyrolysis volatiles, and therefore reduces H_2 production compared to the conventional steam reforming process [57]. It should be highlighted that studies in the literature dealing with this novel strategy, i.e., waste pyrolysis and in-line oxidative steam reforming (P-OSR), are even scarcer than those related to P-SR. To our knowledge, the only reference is that by Czernik and French [48], who operated under autothermal conditions in the reforming step.

Our research team proposed a combination of a conical spouted bed reactor (CSBR) and a fluidized bed reactor (FBR) for the continuous pyrolysis and in-line steam reforming of waste plastics and demonstrated the potential of this strategy for H_2 production [49,58]. This study aims at progressing towards the development and scaling up of the oxidative steam reforming (OSR) process. Thus, a multi-point O_2 injection system has been developed and fine-tuned to ensure a suitable O_2 distribution in the reforming catalyst bed and avoid hot spot formation. Moreover, this system allows supplying O_2 directly into the catalytic bed, avoiding the pre-combustion of the volatile stream before contacting with the catalyst and promoting the in-situ coke combustion. Furthermore, the role played by the main process conditions (reforming temperature, catalyst space time, steam/plastic (S/P) ratio and equivalence ratio (ER)) was assessed in order to determine the most suitable conditions in the OSR at the initial stage of the process.

2. Experimental

2.1. Materials

HDPE in the form of cylindrical granules with 4 mm mean particle size supplied by Dow Chemicals was used as raw material in this experimental work. The main properties (provided by the supplier) of the HDPE are shown in Table 1. Moreover, to make the HDPE characterization more complete, the higher heating value (HHV) was determined in a differential scanning calorimeter (Setaram TG-DSC-111) and in an isoperibolic bomb calorimeter (Parr 1356).

ReforMax® 330 commercial catalyst provided by Süd Chemie was used in the reforming step, which is composed of 14 wt% NiO supported on calcium aluminate. This catalyst has been extensively used in the CH_4 steam reforming, and its suitable activity has been proven in previous P-SR studies [59,60]. Moreover, its selection was motivated by its availability, as well as the avoidance of reproducibility problems involving its synthesis. As the supplied catalyst had a 10-hole ring shape, it was ground and sieved to 0.4–0.8 mm particle size and rounded before the experiments. According to a previous study [58], the selection of this particle size ensures a satisfactory fluidization regime in the FBR. The reforming catalyst was characterized by Brunauer–Emmett–Teller (BET) and temperature programmed reduction (TPR) analysis. The experimental conditions used and the procedure followed in these techniques are detailed elsewhere [61,62]. BET analysis under liquid N_2 (Micromeritics ASAP 2010) revealed that the catalyst has a surface area of 19 $m^2\ g^{-1}$ and an average pore diameter of 122 Å. Besides, the TPR analysis (AutoChem II 2920 Micromeritics) showed two main peaks: the first main one located at 550 °C is related to the reduction of NiO interacting with α-Al_2O_3, and the second one located at 700 °C is attributed to $NiAl_2O_4$. Therefore, 710 °C was selected as the optimum temperature to reduce the catalyst before the pyrolysis-reforming runs. The catalysts reduction was carried out in-situ by feeding a 10 vol% H_2 stream for 4 h.

Silica sand (99 wt% SiO_2) supplied by Minerals Sibelco was used as in-bed material in the CSBR, and also mixed with the reforming catalysts in the fluidized bed reactor. A particle size in the 0.2–0.3 mm range was used in the CSBR, whereas a wider range (0.3–0.35 mm) was used in the FBR.

2.2. Experimental equipment

The P-OSR runs were carried out in continuous mode in a bench scale unit made up of a CSBR and a FBR connected in-line one after the other.

Table 1
HDPE characterization.

Main properties	
Average molecular weight (kg mol^{-1})	46.2
Polydispersity	2.89
Density (kg m^{-3})	940
HHV (MJ kg^{-1})	43

Thus, plastics pyrolysis was carried out in the first reactor, whereas the volatile stream released in the pyrolysis step was reformed under oxidative environment in the second one. Both reactors and the interconnecting pipes were placed into a hot box kept at 300 °C in order to avoid the condensation of the pyrolysis volatiles. Moreover, the reactors are located within independent radiant ovens, which provide the heat required to reach the corresponding reaction temperatures.

The scheme of the bench scale plant used for plastic P-OSR is shown in Fig. 1. This plant was fine-tuned and optimized based on the previous experience of the research group [58,61,63,64]. Furthermore, as the CSBR is characterized by a vigorous movement of bed particles as well as high heat and mass transfer rates, allows minimizing bed agglomeration problems caused by fused plastics and ensures the production of a homogeneous composition stream throughout time [65]. The dimensions of the CSBR can be found elsewhere [58]. Furthermore, unlike previous plastic waste P-SR studies [49,52,63,66], the CSBR was equipped with a non-porous draft tube to improve the stability of the spouting regime, which also allows controlling the bed material circulation and operate with lower gas flow rates [67–71]. The draft tube was designed according to previous hydrodynamic studies carried out by Cortazar et al. [72], with its dimensions being 8 mm in diameter, 5.5 mm gas inlet diameter, 15 mm entrainment zone height and 89 mm total height. Furthermore, the use of a FBR for the reforming step avoids severe coke formation and bed blockage, which are the main problems when fixed beds are used [61,73]. However, the novelty of this study is associated with the injection of O_2 into the volatile reforming unit. Thus, a new multi-point injection device has been developed. As shown in Fig. 2, this device was placed just above the distributor plate in the FBR and enabled feeding O_2 directly into the bed. The stream made up of pyrolysis volatiles and steam enters the reforming reactor through the distributor plate, whereas the O_2 enters through the multi-point feeder. This device not only prevents the volatile stream from pre-oxidation prior to reforming, but also avoids hot spot formation, which may cause the sintering or oxidation of the metallic active phase of the catalyst due to the non-homogeneous distribution of O_2. Moreover, this device guarantees that the heat released in the oxidation reactions is delivered directly to the reforming step.

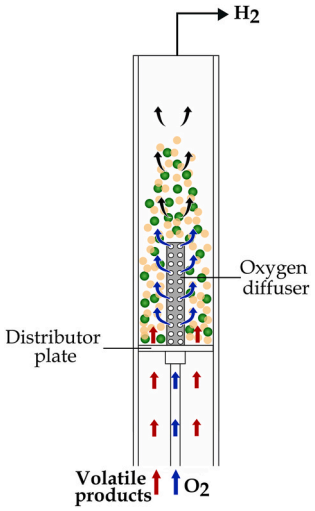

Fig. 2. Scheme of the FBR with the multi-point O_2 injector.

Apart from the reaction system, this bench scale plant is made up of devices for feeding the solid, water and gas, and a product separation section. The plastic was continuously dosed using a vibratory piston feeder, which pushes the plastic towards the top of the vessel and makes it overflow through a cooled tube into the CSBR. This double-shell water cooler connects the feeder and the reactor in order to avoid melting of the plastic, and therefore blocking of the feeding tube. More details about the solid feeding system were reported by Cortazar et al. [74]. As steam was employed as both spouting and fluidizing agent, water was fed by means a peristaltic pump (Gilson 307) and vaporized in an evaporator located below the pyrolysis reactor. Moreover, N_2 (for preheating) and H_2 (for reducing the reforming catalyst before each run) were fed through the bottom of the pyrolysis reactor, where a gas preheater is welded. The gas preheater ensures the gas stream reaches the operation temperature. In the case of O_2, it is directly introduced into the FBR. Finally, the product separation system consists of a filter (placed in

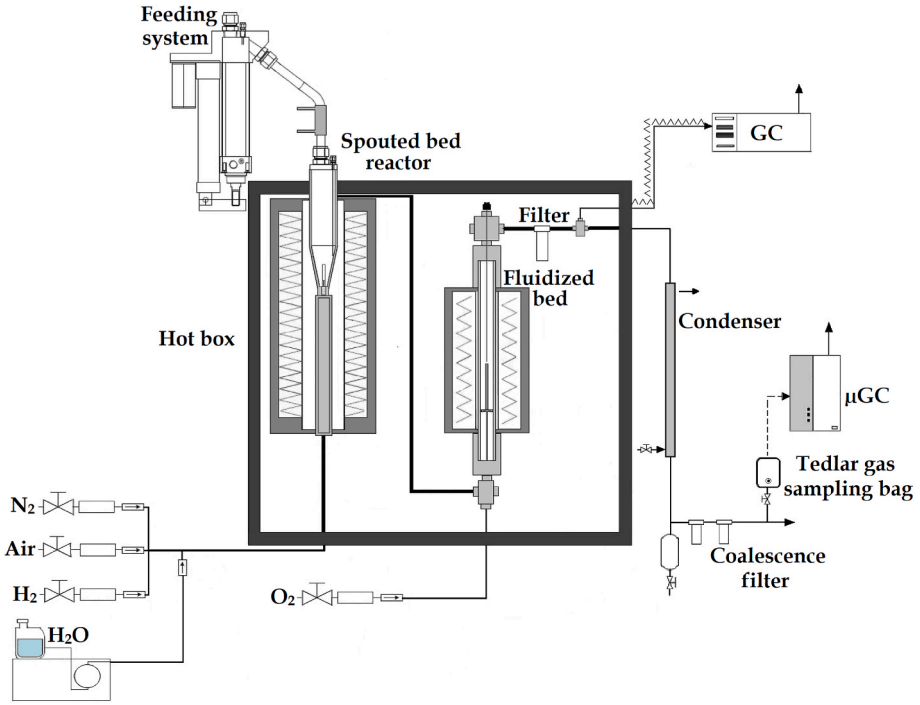

Fig. 1. Scheme of the pyrolysis and in-line oxidative steam reforming bench scale plant.

the hot box, downstream the FBR) to collect the fine catalyst particles formed by attrition and entrained from the bed, a condenser and a coalescence filter.

2.3. Operation conditions and products analysis

Pyrolysis-oxidative steam reforming runs were carried out in continuous regime by feeding 1 g min^{-1} of HDPE. Although different operation conditions were used in each step (reactor), it is to note that steam acts as spouting and fluidizing agent in both reactors. In fact, Erkiaga et al. [61] determined the inert behaviour of steam on plastic pyrolysis at moderate temperatures. Accordingly, the most suitable bed mass and particle size was independently chosen for each bed to ensure joint stable operation under spouting (first step) and fluidization (second step) regimes. Thus, a flow rate of 3 mL min^{-1} of water (3.73 NL min^{-1} of steam) was used for achieving suitable regimes in both steps. Moreover, 75 g of sand (0.2–0.3 mm particle size range) were used in the CSBR and 25 g of reforming catalyst-sand mixture (0.4–0.8 mm and 0.3–0.35 mm size ranges for the catalyst and sand, respectively) in the FBR. The pyrolysis step was performed at 550 °C in all the runs because the bio-oil yield is maximized at this temperature [65]. The HDPE pyrolysis products under N_2 atmosphere were identified and quantified at 550 °C by Elordi et al. [65], and lumped into four main fractions: i) gas (2.4 wt%), ii) gasoline (6.7 wt%), iii) diesel (30.0 wt%) and iv) waxes (60.9 wt%).

Regarding the operating conditions used in the fluidized bed reactor, a detailed parametric study was conducted (Table 2) by changing them as follows: temperature between 550 and 750 °C, S/P ratio between 2 and 5, space time in the 3.12–15.62 g_{cat} min g_{HDPE}^{-1} range and ER in the 0–0.3 range. The S/P ratio was defined as the ratio between the steam and plastic flow rates fed into the pyrolysis step, whereas the ER was defined based on the stream of volatiles fed into the reforming step, i.e., the ratio between the flow rate of O_2 injected and that required for stoichiometric combustion of the volatile stream according to Eq. (1).

$$C_nH_m + \left(\frac{2n + m/2}{2}\right)O_2 \rightarrow nCO_2 + (m/2)H_2O \quad (1)$$

Given the pyrolysis conditions used in this study, all pyrolysis products were volatile compounds and they were transferred into the reforming reactor, i.e., no significant solid residue was retained in the pyrolysis reactor. Therefore, the elemental composition of the pyrolysis volatiles is the same as that of the HDPE in the feed.

All the operating conditions have been established to avoid any operational problems associated with low conversion of waxes at the initial stage.

The analysis of the product stream was conducted in the first stage of the reaction once steady state conditions had been achieved in the process, i.e., after few minutes of operation (about 5 min). All the process products were analyzed by chromatographic techniques. On the one hand, Agilent GC-6890 equipped with a HP-Pona column and flame ionization detector (FID) was used in-line to quantify the amount of volatiles remained after the reforming step. Thus, a sample of the volatile stream was injected into the GC during the operation by means of a line thermostated at 220 °C. On the other hand, the permanent gases generated were collected downstream in a Tedlar bag. These gases were analyzed subsequently off-line in an Agilent 4900 micro-GC containing three analytical modules (MS5A, Plot-Q and Plot-Al_2O_3) and their corresponding thermal conductivity detectors (TCD). All the analyses were repeated at least three times under the same experimental conditions to ensure reproducibility of the results and determine average values within a short range (below 5 %) with 95 % confidence interval.

Table 2
Experimental conditions in the parametric study of the oxidative steam reforming step.

Temperature (°C)	550, 600, 650, 700, 750 (space time: 12.5 g_{cat} min g_{HDPE}^{-1}; S/P: 3; and ER: 0.2).
Space time (g_{cat} min g_{HDPE}^{-1})	3.12, 6.25, 12.5, 15.62 (T: 700 °C; S/P: 3 and ER: 0.2).
S/P ratio	2, 3, 4, 5 (T: 700 °C; space time: 12.5 g_{cat} min g_{HDPE}^{-1} and ER: 0.2).
ER	0, 0.1, 0.2, 0.3 (T: 700 °C; space time: 12.5 g_{cat} min g_{HDPE}^{-1} and S/P: 3).

2.4. Reaction indices

In order to assess process performance, the conversion and individual product yields were considered. The following reaction indices were defined:

The conversion of the volatiles (X, %) (Eq. (2)) is the ratio between the moles of C recovered in the gaseous product stream and those in the plastic pyrolysis volatile stream fed into the reforming reactor. As aforementioned, the flow rate of the volatile stream fed into the reforming reactor is the same as that of the HDPE fed into the pyrolysis reactor because no solid residue is retained in the pyrolysis step.

$$X_{HDPE} = \frac{C_{gas}}{C_{volatiles}} \cdot 100 \quad (2)$$

The individual products yields (Y_i, %) (only those containing C) are considered by Eq. (3):

$$Y_i = \frac{F_i}{F_{volatiles}} \cdot 100 \quad (3)$$

where F_i is the molar flow rate of each *i* carbon compound and $F_{volatiles}$ the flow rate of HDPE pyrolysis volatile compounds. Moreover, the gaseous stream is made of CO, CO_2, CH_4, and C_2–C_4 hydrocarbons, as well as non-converted pyrolysis volatiles consisting of C_{5+} hydrocarbons.

The hydrogen yield (Y_{H2}, %) was expressed (Eq. (4)) as the ratio between the molar flow rate of H_2 (F_{H2}) and the maximum allowable by stoichiometry (F_{H2}^0) in the pyrolysis-oxidative reforming reaction given by Eq. (5):

$$Y_{H_2} = \frac{F_{H_2}}{F_{H_2}^0} \cdot 100 \quad (4)$$

$$C_nH_m + \alpha O_2 + (2n\text{-}2\alpha)H_2O \rightarrow nCO_2 + (2n - 2\alpha + m/2)H_2 \quad (5)$$

where $\alpha = 0$ is when no O_2 is used; that is, under steam reforming (SR) conditions.

Specific gas yield (Y_{gas}, m^3 kg^{-1}) was defined by mass unit of HDPE in the feed in the pyrolysis reactor (Eq. (6)).

$$Y_{gas} = \frac{Q_{gas}}{m_{HDPE}^0} \cdot 100 \quad (6)$$

where Q_{gas} is the volumetric flow rate of the produced gases and m_{HDPE}^0 is the mass flow rate of HDPE fed into the process.

Finally, the H_2 production (Prod. H_2, wt%) was quantified by mass unit of the HDPE in the feed (Eq. (7)):

$$\text{Prod. } H_2 = \frac{m_{H_2}}{m_{HDPE}^0} \cdot 100 \quad (7)$$

where m_{H2} is the mass flow rate of H_2 produced in the process.

3. Results

The influence of the main process conditions, i.e., temperature, space time, S/P and ER ratios, was evaluated to assess their effect on the conversion, products yields and gaseous stream composition at the initial reaction stage. Thus, several reactions have been considered to explain the results obtained in the plastic P-OSR process, such as

methane steam reforming (Eq. (8)), hydrocarbons steam reforming (Eq. (9)), water gas shift (WGS) (Eq. (10)), methane dry reforming (Eq. (11)), hydrocarbons dry reforming (Eq. (12)), hydrogen oxidation (Eq. (13)), methane oxidation (Eq. (14)), hydrocarbons oxidation (Eq. (15)) and carbon monoxide oxidation (Eq. (16)).

$$CH_4 + H_2O \leftrightarrow CO + 3H_2 \quad (8)$$

$$\text{Hydrocarbons} + H_2O \rightarrow CO + H_2 \quad (9)$$

$$CO + H_2O \leftrightarrow CO_2 + H_2 \quad (10)$$

$$CH_4 + CO_2 \leftrightarrow 2CO + 2H_2 \quad (11)$$

$$\text{Hydrocarbons} + CO_2 \rightarrow CO + H_2 \quad (12)$$

$$H_2 + \frac{1}{2}O_2 \rightarrow H_2O \quad (13)$$

$$CH_4 + 2O_2 \rightarrow CO_2 + 2H_2O \quad (14)$$

$$\text{Hydrocarbons} + O_2 \rightarrow CO_2 + H_2O \quad (15)$$

$$CO + \frac{1}{2}O_2 \rightarrow CO_2 \quad (16)$$

It should be highlighted that this is a very novel strategy for H_2 production from waste plastics. Given the lack of similar studies involving waste plastics P-OSR published in the literature, the data used for comparison with the results obtained in this study correspond mostly to the OSR of model hydrocarbons obtained in the pyrolysis of plastics.

3.1. Effect of temperature

A suitable choice of process parameters and understanding their role in the P-OSR is essential for scaling up this process. Thus, the influence of the reforming temperature was analyzed from 550 to 750 °C using a S/P ratio of 3, space time of 12.5 g_{cat} min g_{HDPE}^{-1} and ER of 0.2. It is to note that, according to a previous thermodynamic equilibrium simulation study [75], an ER of 0.2 corresponds to autothermal operation in the reforming step. In the OSR process, the volatile fraction from HDPE pyrolysis is broken down and converted into gases. This gaseous stream is mainly made up of H_2, CO_2, CO, CH_4 and light hydrocarbons (mostly ethylene, ethane, propylene and propane). Moreover, the non-reformed liquid fraction was lumped into the C_5^+ fraction.

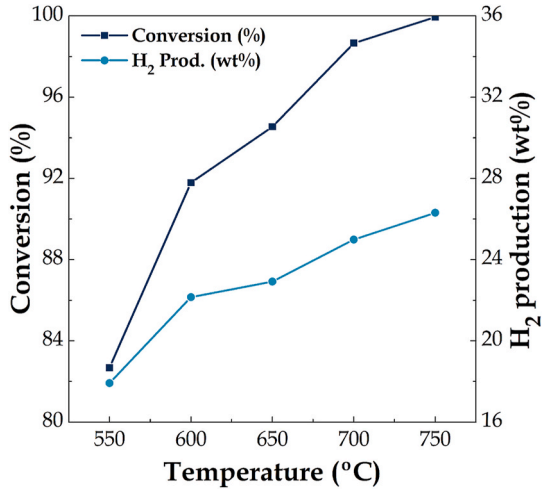

Fig. 3. Effect of the reforming temperature on HDPE conversion and H_2 production. Oxidative reforming conditions: space time, 12.5 g_{cat} min g_{HDPE}^{-1}; S/P ratio, 3; and ER, 0.2.

Fig. 3 shows the conversion of HDPE volatiles and H_2 production in the OSR process at different temperatures. Under autothermal operation, a temperature increase from 550 to 750 °C improved the conversion of HDPE volatiles from 82.7 to 99.9 %, which is evidence that almost full conversion of waxes and diesel fraction into the gaseous fraction was attained (Fig. 4a). These results are also a proof of the high initial activity of the catalyst used in this study for the OSR of HDPE pyrolysis volatile compounds. It is well-known that an increase in temperature improves reforming and partial oxidation reaction rates (Eqs. (8–16)). Thus, at the lower temperature studied, 550 °C, a considerable yield of non-converted gaseous (methane and C_2–C_4) and liquid (C_5^+) hydrocarbons was observed, but higher temperatures led to their reforming, with the yield of C_2–C_4 and C_5^+ fractions being negligible at 750 °C.

Barbarias et al. [58] conducted the pyrolysis and in-line conventional steam reforming at 700 °C, and obtained a conversion of 98 %, which is slightly lower than that obtained in this study (98.7 %) under autothermal conditions. Moreover, it should be noted that the previous study [58] was conducted at more favourable process conditions, i.e., higher space time (16.7 g_{cat} min g_{HDPE}^{-1}) and higher S/P (a value of 4), which is evidence of the benefits of autothermal operation.

Kang and Bae [76] analyzed the effect of temperature from 700 to 900 °C on the autothermal reforming of hexadecane to produce diesel surrogate and reported that 750 °C was enough for attaining almost full fuel conversion on noble metal catalysts. However, the same research group [77] reported that higher temperatures (about 800 °C) are needed for full conversion of isooctane, which was used as gasoline surrogate. According to Palm et al. [78], C–C bond energies are usually stronger in aromatic compounds than in paraffins, which makes the former more difficult to convert. Thus, the different reactivity of diverse model compounds, namely, a short paraffin (n-hexane), an olefin (1-hexene), a long paraffin (tetradecane) and an aromatic compound (toluene), was assessed in the steam reforming conducted at 700 °C [66]. It was concluded that aromatic compounds are less reactive than linear hydrocarbons. Furthermore, reaction rates are lower as the chain of the linear hydrocarbons is longer. However, the overall reactivity of the fuels is difficult to predict from the results of individual model compounds [79], since their reforming behaviour may differ when they are alone or are part of the HDPE pyrolysis stream due to the interactions that may occur between components.

Likewise, H_2 production was also significantly enhanced from 17.9 to 26.3 wt%, as reforming reactions (Eqs. (8-12))) were favoured with temperature and plastics derived volatiles were fully converted. The same trend was observed by Alvarez-Galvan et al. [80] for H_2 production in the OSR of diesel surrogate (a mixture of n-hexadecane, decaline and tetracaline in similar proportion as in the diesel fraction) when increasing the temperature from 750 to 850 °C. Although Alvarez-Galvan et al. [80] found higher H_2 production at 850 °C, they chose 800 °C as the optimum one in order to keep moderate activity levels allowing discrimination between different catalysts.

The influence of the reforming temperature on the yields of the gaseous products and their concentrations are shown in Fig. 4. H_2 yield is based on the maximum allowable by stoichiometry, whereas the yields of carbonaceous compounds are based on the moles of carbon in the HDPE. The evolution of the products yields can be explained by the effect of temperature on the steam reforming (Eqs. (8),(9)) and WGS (Eq. (10)) reactions. As steam reforming reactions (Eqs. (8),(9)) are highly endothermic, they are shifted towards the formation of H_2 and CO when reforming temperature is raised. However, the opposite is expected for the exothermic WGS reaction (Eq. (10)). Thus, the production of CO and H_2O is favoured at high temperatures at the expense of consuming H_2 and CO_2. As observed, temperature played a positive role in H_2 yield (based on the maximum allowable by stoichiometry), increasing from 58.3 % at 550 °C to 76.4 % at 750 °C. Moreover, the production of CO was also enhanced with temperature, yielding 49.0 % at 750 °C. These results are evidence that reforming reactions prevail at high

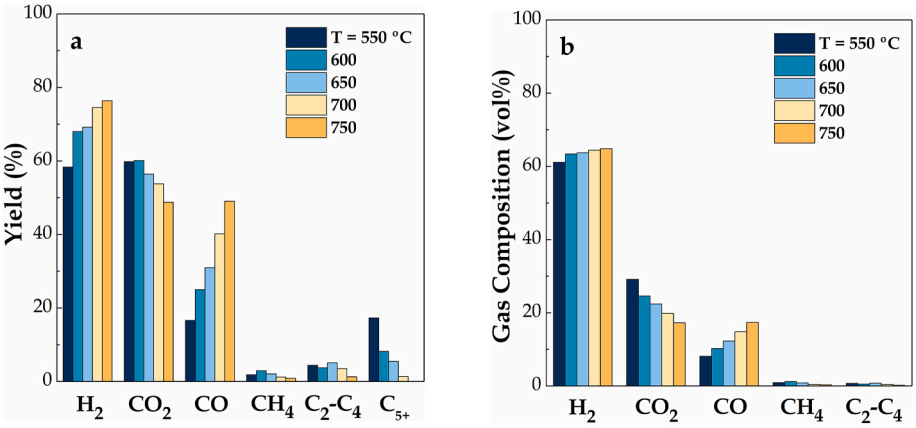

Fig. 4. Effect of the reforming temperature on the yields of gaseous product (a) and their concentration (b). Oxidative reforming conditions: space time, 12.5 g_{cat} min g_{HDPE}^{-1}; S/P ratio, 3; and ER, 0.2.

temperatures (Eqs. (8),(9)). In the case of CO_2, it decreased from 59.8 to 48.8 % with temperature due to the enhancement of the reverse WGS reaction. Promotion of reforming reactions (Eqs. (8),(9)) with temperature can also be observed in view of CH_4, C_2–C_4 and C_{5+} fractions, which were considerably reduced. Thus, a considerable yield of C_{5+} fraction was obtained at 550 °C (17.3 %), but this fraction was almost fully converted by increasing temperature to 750 °C at the expense of increasing H_2 and CO yields.

The influence of temperature on the concentrations of gaseous components (Fig. 4b) followed the same trend as for the individual yields (Fig. 4a); that is, H_2 and CO concentrations decreased, whereas that of CO_2 increased when reforming temperature was raised from 550 to 750 °C. However, it can be observed that the effect of temperature on H_2 concentration is rather limited, as it slightly increased from 61.1 to 64.9 vol%. A greater effect was noticed for CO and CO_2 concentrations, i.e., CO concentration increased from 8.1 to 17.4 vol%, whereas that of CO_2 decreased from 29.2 to 17.3 vol%. These results are evidence that the WGS reaction (Eq. (10)) is not thermodynamically favoured at high temperatures. Kang and Bae [76] reported H_2, CO and CO_2 concentrations of 58, 22 and 18 vol% respectively, at 750 °C in the OSR of hexadecane, which were quite similar to those obtained in this work. Moreover, these results are consistent with the results reported by other authors in continuous [47,81,82] or batch [83–85] P-SR of different plastic wastes when temperature was increased.

The selection of a suitable temperature for OSR is extremely important. Thus, temperature not only has a positive effect on HDPE volatile conversion and H_2 production, but is also closely related to the energy demand of the process and the stability of the catalyst [75]. High temperatures lead, on the one hand, to lower deactivation rates and coke deposition [52], but, on the other hand, they may contribute to sintering [36]. Thus, the operating temperature range should strike a balance between the previous factors. In this case, as Ni-based catalyst is used in the reforming step, 700 °C has been established as the optimum temperature for the OSR of HDPE volatiles.

3.2. Influence of space time

The effect of the space time on the process was analyzed in the range of 3.12–15.62 g_{cat} min g_{HDPE}^{-1}. The runs were conducted at autothermal regime (ER = 0.2) with the reforming temperature being set at 700 °C and the S/P ratio at 3. Fig. 5 shows that the conversion of HDPE volatiles and H_2 production were significantly improved by increasing space time, i.e., from 91.1 to 98.6 % and from 12.5 to 25.4 wt%, respectively. However, a further increased from 12.5 to 15.62 g_{cat} min g_{HDPE}^{-1} hardly improved the results because operation was being conducted close to thermodynamic equilibria. The saturating trend of conversion when the

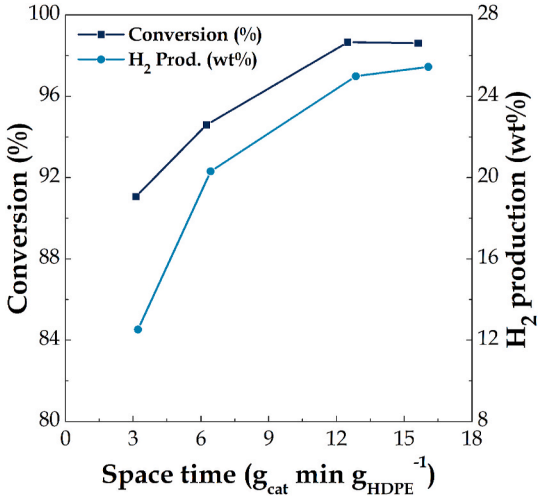

Fig. 5. Effect of space time on HDPE conversion and hydrogen production. Oxidative reforming condition: 700 °C; S/P ratio, 3; and ER, 0.2.

amount of catalyst was increased is also consistent with the results reported by Khan et al. [86] in the oxidative reforming of synthetic diesel on a Ni-based catalyst. Likewise, Barbarias et al. [58] observed the same effect on the steam reforming of HDPE volatiles. Under similar operating conditions (T = 700 °C, space time of 12.5 g_{cat} min g_{HDPE}^{-1} and S/P = 4) the previous authors reported a conversion of 97.5 %, which was slightly lower than that obtained under autothermal conditions (98.7 %).

It is to note that a specific gas production of 4.4 Nm^3 kg^{-1} was obtained when the operation was conducted with a space time of 15.62 g_{cat} min g_{HDPE}^{-1}, which is evidence of the efficiency of the two-step process of HDPE pyrolysis and in-line oxidative reforming in comparison with other thermochemical conversion routes in which plastic wastes are valorized. Thus, gas yields in the range of 1.2–3.4 Nm^3 $kg_{plastic}^{-1}$ have been reported under optimum operating conditions in the waste plastics steam gasification [87–89].

The influence of space time on product yields is shown in Fig. 6a. The use of high space times, i.e., large amounts of catalyst, promoted steam reforming and WGS reactions (Eqs. (8-10)), leading to an increase in H_2, CO_2 and CO yields and a decrease in those of CH_4, C_2–C_4 and C_{5+}. Although reductions are evident for C_2–C_4 and C_{5+} yields, especially for the former, which decreased by 93 %, this effect was much less pronounced in the CH_4 yield. These results confirmed the suitability of this catalyst for enhancing reforming and WGS reactions (Eqs. (8-10)).

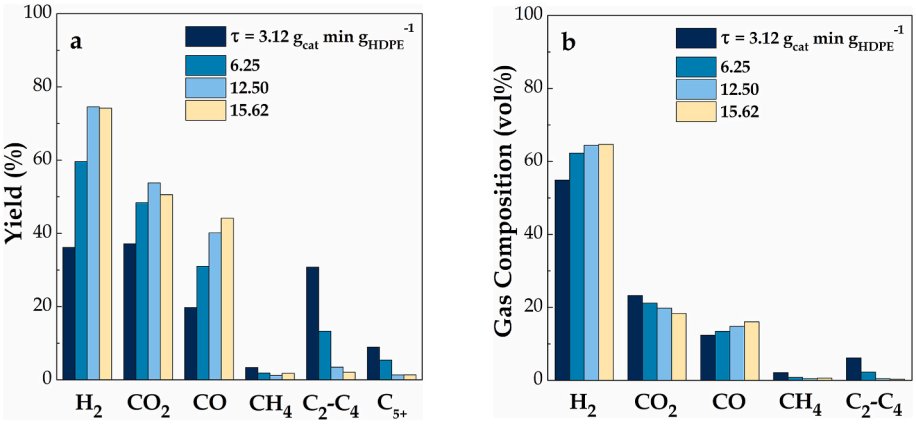

Fig. 6. Effect of reforming space time on the yields of gaseous products (a) and their concentrations on the gas fraction (b). Oxidative reforming condition: 700 °C; S/P ratio, 3; and ER, 0.2.

Regarding the concentrations of gaseous components (Fig. 6b), the same trend as for the products yields was observed when increasing space time, except for CO_2 concentration, which declined. It seems that dry reforming reactions (Eqs. (11),(12)) may also be favoured at high space times. Thus, an increase in space time to 15.62 g_{cat} min g_{HDPE}^{-1} led to an increase in H_2 and CO concentrations, from 54.9 and 12.4 to 64.7 and 16.1 vol%, respectively, and a decrease in that of CO_2, from 23.3 to 18.4 vol%. A similar trend was also reported by Shilov et al. [90] when increasing the amount of catalyst in the OSR of hexadecane or diesel model blends.

3.3. Influence of steam/plastic (S/P) ratio

The influence of steam partial pressure on the reaction environment was analyzed using S/P ratios from 2 to 5. The other operating conditions were as follows: temperature 700 °C, space time 12.5 g_{cat} min g_{HDPE}^{-1} and ER = 0.2. An increase in S/P ratio had a positive effect on both HDPE volatile conversion and H_2 production (Fig. 7). Thus, the volatile conversion increased from 96.5 to 99.9 % in the studied S/P ratio range. However, for S/P ratios of 3 or higher, the effect of steam partial pressure was rather limited, as almost full conversion (above 98 %) was achieved under those cases. These results are evidence that a S/P ratio of 3 provided enough amount of steam for converting HDPE volatiles through reforming reactions. Moreover, it should be pointed out that O_2 addition also contributed to the conversion of HDPE volatiles, which required lower amounts of steam for full conversion. In other words, although higher steam concentrations improve the reforming performance, O_2 co-feeding reduces the steam required in the reforming step to reach full conversion of the HDPE volatiles. This effect is noticeable when comparing the conversion obtained in this study (98.7 %) under autothermal operation with that by Barbarias et al. [58], who reported a volatile conversion below 98 % using a higher amount of catalyst (700 °C, a space time of 16.7 g_{cat} min g_{HDPE}^{-1} and a S/P ratio of 3).

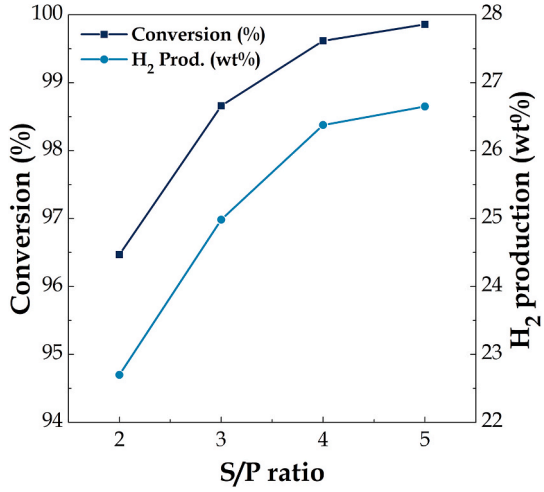

Fig. 7. Effect of S/P ratio on HDPE conversion and H_2 production. Oxidative reforming conditions: 700 °C; space time (g_{cat} min g_{HDPE}^{-1}), 12.5; and ER, 0.2.

An increase in the steam partial pressure increases the rate of both reforming and WGS reactions (Eqs. (8-10)). Moreover, the equilibrium of the latter reaction is also shifted towards H_2 formation. These effects are evidenced by the higher conversion and H_2 production (increasing from 22.7 to 26.6 wt% in the range studied). Unlike volatile production, for which a S/P ratio of 3 was enough to attain almost full conversion, a S/P ratio of 4 showed an additional 5 % increase in H_2 production. For S/P ratios higher than 4, the beneficial effect of steam partial pressure on H_2 production is rather limited. The positive effect on H_2 production by increasing the S/C ratio was also reported by Alvarez-Galvan et al. [80], who noticed that although S/C ratios higher than the stoichiometric ones are recommended for enhancing the reforming of heavy hydrocarbons, very high S/C ratios hardly improved H_2 production.

The same trend was also observed for the products yields (Fig. 8a). Similarly to H_2 production, H_2 yield also increased, as well as that of CO_2, due to the enhancement of reforming and WGS reactions (Eqs. (8-10)).. Thus, for a S/P ratio of 5, H_2 and CO_2 yields were 83.5 and 68.5 %, respectively. However, the yields of CO, CH_4 and other hydrocarbons decreased when S/P ratio was increased. Thus, the CO yield decreased by around 40 %, whereas those of CH_4 and other hydrocarbon were almost negligible.

Fig. 8b shows the effect of S/P ratio on the concentration of gaseous components. A similar trend as for the products yields was observed for the composition of the gas. Thus, similarly to H_2 yield, the H_2 concentration also increased, but more smoothly, from 62.8 to 65.4 vol%. In the case of CO_2 and CO concentrations in the gas, a more remarkable effect could be noticed as S/P ratio was increased. Thus, for a S/P of 5, CO_2 concentration increased to 24.0 vol%, whereas that of CO declined to 10.2 vol%. Regarding the concentrations of CH_4 and other light hydrocarbons in the gaseous stream, their significance is very low. An increase in H_2 and CO_2 concentrations and a decrease in that of CO was also noticed by several authors in the OSR of a vacuum residue [91], hexadecane [76,80] and n-dodecane [92,93]. Besides, the same qualitative effect of S/P ratio, i.e., an increase in H_2 and CO_2 yields as S/P is increased, was observed in the steam reforming of plastics pyrolysis volatiles [58,84,94,95]. Moreover, an increase in S/P ratio also leads to an increase in the water reacted during the process. Thus, for a S/P ratio of 2, the water reacted accounts for 934.1 g kg_{HDPE}^{-1}, with this value being considerably higher when a S/P ratio of 5 was used (1341.8 g kg_{HDPE}^{-1}).

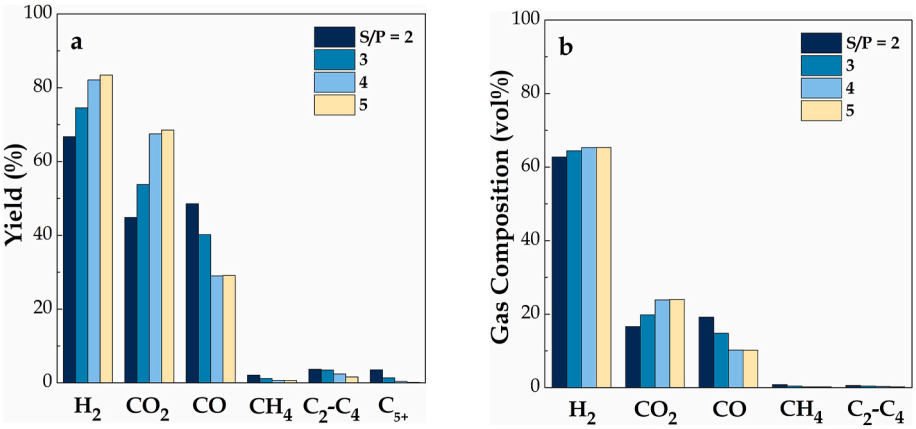

Fig. 8. Effect of S/P ratio on the yields of gaseous products (a) and their concentration on the gas fractions (b). Oxidative reforming condition: 700 °C; space time (g_{cat} min g_{HDPE}^{-1}), 12.5; and ER, 0.2.

From these results, it is clear that high S/P ratios favour the process of waste plastics P-OSR, attaining almost full conversion of HDPE volatiles and high H_2 productions, of around 25–26 wt%. Moreover, according to several authors [52,96,97], high S/P ratios could help preventing carbon deposition on the catalyst. However, this ratio should be carefully selected, as a high S/P ratio can lower the energy efficiency of the process. In fact, the energy requirements associated with water vaporization, heating and condensation are extremely high. Therefore, it is necessary to strike a balance between H_2 production and energy efficiency of the process. In view of the obtained results, a S/P ratio of 3 has been selected as the optimum one.

3.4. *Influence of ER*

The effect of the ER ratio was studied between 0 and 0.3, with the remaining operating conditions being as follows: 700 °C, a space time of 12.5 g_{cat} min g_{HDPE}^{-1} and a S/P ratio of 3. It should be noted that O_2 incorporation into the reforming step greatly modifies the overall enthalpy of the process. As mentioned before, a previous study [75] approached under thermodynamic equilibrium showed that an ER = 0.2 is enough for autothermal operation with S/P ratios above 2. However, reaction enthalpy for conventional steam reforming (ER = 0) of HDPE pyrolysis volatiles is above 9 MJ kg_{HDPE}^{-1}. Based on the results obtained in the aforementioned thermodynamic simulation [75], the ER values selected in this study range from those below autothermal operation (endothermic) to those above autothermal operation (exothermic). Furthermore, ER = 0 corresponding to pure steam reforming conditions was tested for comparison purposes.

Fig. 9 shows the effect of O_2 co-feeding on the HDPE volatiles conversion and H_2 production. On the one hand, an increase in ER led to an improvement in the conversion of the volatiles due to the higher extent of oxidation reactions (Eqs. (13-15)). . Thus, an increase in ER from 0 to 0.3 entailed an increase in conversion from 96.3 % to almost full conversion of the volatiles (99.3 %). On the other hand, O_2 incorporation has a detrimental effect on H_2 production as H_2 partial oxidation reactions (Eq. (13)) were enhanced, which caused a decrease in hydrogen production from 27.9 wt% (steam reforming conditions) to 21.9 wt% (oxidative steam reforming conditions).

An increase in ER caused a significant increase in H_2, CO_2 and CO yields, whereas those of CH_4, C_2–C_4 and C_{5+} fractions declined (Fig. 10a). The opposite trends observed for H_2 production and yield are related to the calculation basis. It should be noted that, unlike H_2 production, which is based on the amount of plastic in the feed, H_2 yield is defined as a percentage of the maximum allowable by stoichiometry (Eq. (5)), which decreases as ER is increased. Therefore, H_2 yield varies depending on the amount of O_2 introduced in the reforming step, as well as on the yields of non-converted CH_4, C_2–C_4 and C_{5+} fractions. That is, as ER is increased, the amount of non-converted compounds decreases, and therefore, H_2 yield increases.

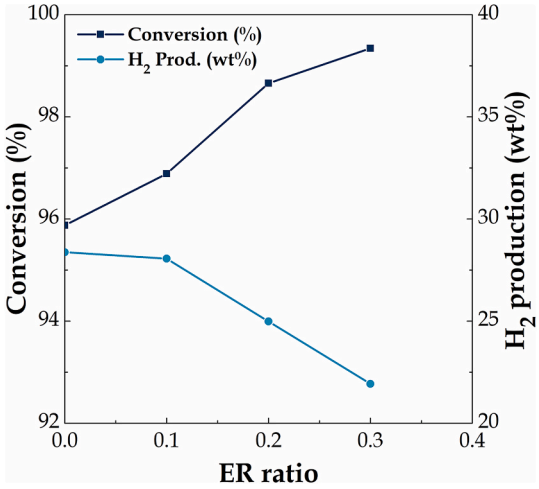

Fig. 9. Effect of ER on HDPE conversion and H_2 production. Oxidative reforming conditions: 700 °C; space time (g_{cat} min g_{HDPE}^{-1}), 12.5; and S/P ratio, 3.

Thus, a H_2 yield of 65.9 % was obtained under steam reforming conditions, whereas this value peaked at 74.6 % when using an ER = 0.2. Higher ER values did not show a major change in the H_2 yield, i.e., a similar value is obtained at ER = 0.3. Regarding the CO_2 yield, its increase from 43.6 to 57.2 % is strongly associated with the enhancement of CH_4 and volatile oxidation reactions (Eqs. (14),(15)) when the amount of O_2 in the feed is increased. Consequently, a significant reduction in the yields of carbon containing compounds except CO_2 was noticed, especially in those of CH_4 and C_{5+} fractions, which were almost completely converted. In the case of CO yield, an interesting trend was observed. As a higher O_2 amount was incorporated into the reforming step (until autothermal operation was reached), CO_2 formation was favoured, and therefore dry reforming reactions (Eqs. (11),(12)) involving methane and volatiles were also enhanced, causing an increase in the CO yield. However, when the overall reforming reaction was exothermic (ER > 0.2), CO oxidation reaction (Eq. (16)) was favoured, and therefore CO yield was reduced in benefit of that of CO_2.

Likewise, an increase in ER led to a similar trend for the composition of carbon containing compounds (Fig. 10b); that is, higher CO and CO_2 concentrations and lower of those of CH_4 and light hydrocarbons (related to the enhancement of partial oxidation and dry reforming

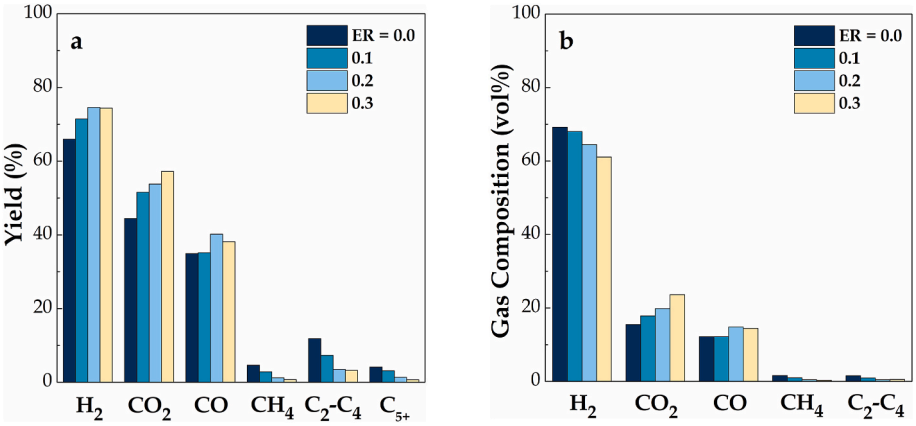

Fig. 10. Effect of ER on the yields of gaseous products (a) and their concentration on the gas fraction (b). Oxidative reforming conditions: 700 °C; space time (g_{cat} min g_{HDPE}^{-1}), 12.5; and S/P ratio, 3.

reactions). Furthermore, the promotion of oxidation reactions (Eqs. (13-16)) at the expense of the reforming ones (Eqs. (8-10)) led to lower H_2 concentration, from 68.6 to 61.1 vol%. Cheekatamarla and Lane [98] conducted oxidative steam reforming of synthetic diesel and reported that H_2 concentration dropped from 60 to 40 vol% when the O_2/C ratio was increased from 0.5 to 2.

Although operating under optimum autothermal conditions lowers H_2 production (in the order of 25.0 wt%) compared to those obtained in the steam reforming of HDPE volatiles (Fig. 9), the results obtained in this study are evidence of the potential of continuous P-OSR of waste plastics. Accordingly, Czernik and French [48] compared P-OSR and P-SR of polypropylene and observed that H_2 production decreased from 34 to 24 wt% under autothermal operation (ER = 0.25). Unlike the previous authors, who conducted continuous operation, as well as Namioka et al. [47,82] and our research group [49,61], the P-SR process has been mostly studied in lab scale units made up of two fixed bed reactors operating in batch regime. Although H_2 productions in the 30–38 wt% range were obtained in the continuous P-SR of different plastic wastes, it should be noted that much lower H_2 productions, in the 7–15 wt% range, were obtained in the P-SR carried out in two fixed bed reactors in series operating in batch mode, as reported by several authors [99–103]. Moreover, P-OSR leads to higher H_2 productions in comparison with optimized steam gasification processes. It should be emphasized that this novel strategy produces a gaseous stream free of tars and overcomes the high energy requirements of the gasification process, with operation being conducted at milder temperatures. Thus, Erkiaga et al. [87] reported a H_2 production of 18 wt% at 900 °C in the HDPE steam gasification and a tar concentration of 16.7 g Nm^{-3}. Furthermore, other authors reported much lower H_2 productions, below 6 wt%, under optimized conditions [88,89,104].

4. Conclusions

The combination of CSBR and FBR technology is suitable for the pyrolysis and in-line oxidative reforming of plastic wastes. Moreover, a multi-point O_2 injection system was developed and fine-tuned to distribute O_2 homogeneously through the catalytic bed in the FBR. Thus, hot spots that may cause irreversible catalyst deactivation by metal sintering, as well as pre-oxidation of the volatile stream before contacting the catalyst, were avoided and in-situ coke combustion was promoted.

The role played by the main operating conditions (temperature, space time, S/P ratio and ER) was assessed for the OSR of HDPE pyrolysis volatiles. An increase in the values of all these variables clearly improved the initial conversion of the plastics derived volatile stream due to several facts, such as increased reaction rates and promotion of reforming and WGS reactions, as well as those involving partial oxidation. Overall, H_2 production was also boosted by increasing the values of the studied variables, except the ER, which caused a significant reduction. Thus, the optimum range of the variables was selected based not only on the HDPE pyrolysis volatiles conversion and H_2 production, but considering also other practical aspects. In the case of the reforming temperature, values as high as 750 °C led to almost full conversion of the volatiles (99.6 %) with high reaction rates and high H_2 production (26.3 wt%). However, 700 °C has been determined as the most suitable temperature because it allows obtaining high conversion of the volatile stream (98.7 %) and H_2 production (25.0 wt%) without endangering the stability of the Ni catalyst due to sintering problems, which may happen with higher temperatures. Regarding the space time, 12.5 g_{cat} min g_{HDPE}^{-1} has been selected as the optimum value, as a further increase to 15.62 g_{cat} min g_{HDPE}^{-1} hardly improved the volatiles conversion and/or H_2 production, likely due to the proximity to thermodynamic equilibria. Based on the results, higher S/P ratios enhanced both volatiles conversion and H_2 production. However, a S/P ratio of 3 has been chosen as the optimum one as it strikes a balance between those indices and the energy efficiency of the process (costs associated with water vaporization are high). Finally, O_2 co-feeding into the FBR caused a decline in H_2 production, with an ER value of 0.2 corresponding to autothermal operation being the optimum one to solve the high energy requirements associated with the high endothermicity of reforming reactions. Thus, under the selected conditions (700 °C, S/P = 3, 12.5 g_{cat} min g_{HDPE}^{-1} and ER = 0.2), almost full initial conversion of the volatiles (up to 98 %) and a H_2 production of 25 wt% was obtained, which was only 28.6 % lower than that obtained under conventional pyrolysis-steam reforming process. These results confirmed the potential of the continuous P-OSR process for the selective production of H_2, which, as aforementioned, can be used for the production of chemicals such as ammonia or methanol, or any form of energy for diverse end-use applications. Furthermore, the operational advantages of P-OSR, i.e., autothermal operation and higher catalyst stability, are crucial facts to be considered in the implementation of this process. Accordingly, future research studies will be guided towards the assessment of catalyst stability, with particular emphasis placing on identifying the main causes and mechanisms of catalyst deactivation for the design of specific catalysts for the process.

CRediT authorship contribution statement

Mayra Alejandra Suarez: Investigation, Data curation. **Katarzyna Januszewicz:** Writing – original draft, Formal analysis. **Maria Cortazar:** Writing – original draft, Formal analysis, Data curation. **Gartzen Lopez:** Writing – review & editing, Validation, Project administration, Funding acquisition. **Laura Santamaria:** Validation, Supervision, Methodology. **Martin Olazar:** Validation, Project administration, Funding acquisition, Writing – review & editing. **Maite Artetxe:**

Funding acquisition, Project administration, Supervision, Writing – review & editing. **Maider Amutio:** Funding acquisition, Project administration, Supervision, Writing – review & editing.

Declaration of competing interest

The authors declare that they have no known competing financial interests or personal relationships that could have appeared to influence the work reported in this paper.

Data availability

Data will be made available on request.

Acknowledgement

This work was carried out with the financial support of the grants PID2022-140704OB-I0 and PID2022-139454OB-I00 funded by MICIU/AEI/10.13039/501100011033 and by "ERDF/EU", the grants TED2021-132056B–I00, PLEC2021-008062 and CNS2023-144031 funded by MICIU/AEI/10.13039/501100011033 and by the "European Union NextGenerationEU/PRTR", and the grants IT1645-22 and KK-2023/0060 funded by the Basque Government. Mayra Suárez also is grateful for the Ph.D. grant PRE2019-088156 funded by MCIN/AEI/10.13039/501100011033 and "ESF :501100023651 Investing in your future".

References

[1] Plastics Europe. Plastics - the facts 2022. 2022.
[2] Burlakovs J, Kriipsalu M, Porshnov D, Jani Y, Ozols V, Pehme K, et al. Gateway of landfilled plastic waste towards circular economy in Europe. Separations 2019;6. https://doi.org/10.3390/separations6020025.
[3] SISTEMIQ. Beaking the plastic waste: a comprehensive assessment of pathways towards ocean plastic polution. 2020.
[4] Wilts H, Bakas I. Preventing plastic waste in Europe. European Environment Agency. Publications Office; 2019. https://doi.org/10.2800/096909.
[5] MacLeod M, Arp HPH, Tekman MB, Jahnke A. The global threat from plastic pollution. Science 2021;373:61–5. https://doi.org/10.1126/science.abg5433.
[6] Borrelle SB, Ringma J, Lavender Law K, Monnahan CC, Lebreton L, McGivern A, et al. Predicted growth in plastic waste exceeds efforts to mitigate plastic pollution. Science 2020;369:1515–8. https://doi.org/10.1126/SCIENCE.ABA3656.
[7] SYSTEMIQ. ReShaping plastics: pathways to a circular, Climate Neutral plastics system in Europe. 2022.
[8] Ragaert K, Delva L, Van Geem K. Mechanical and chemical recycling of solid plastic waste. Waste Manage 2017;69:24–58. https://doi.org/10.1016/j.wasman.2017.07.044.
[9] Kumagai S, Nakatani J, Saito Y, Fukushima Y, Yoshioka T. Latest trends and challenges in feedstock recycling of polyolefinic plastics. J Jpn Petrol Inst 2020;63:345–64. https://doi.org/10.1627/JPI.63.345.
[10] Sharma B, Goswami Y, Sharma S, Shekhar S. Inherent roadmap of conversion of plastic waste into energy and its life cycle assessment: a frontrunner compendium. Renewable Sustainable Energy Rev 2021;146:111070. https://doi.org/10.1016/j.rser.2021.111070.
[11] Rahimi A, Garciá JM. Chemical recycling of waste plastics for new materials production. Nat Rev Chem 2017;1:46. https://doi.org/10.1038/s41570-017-0046.
[12] Thiounn T, Smith RC. Advances and approaches for chemical recycling of plastic waste. J Polym Sci 2020;58:1347–64. https://doi.org/10.1002/pol.20190261.
[13] Gluth A, Xu Z, Fifield LS, Yang B. Advancing biological processing for valorization of plastic wastes. Renewable Sustainable Energy Rev 2022;170:112966. https://doi.org/10.1016/j.rser.2022.112966.
[14] Dogu O, Pelucchi M, Van de Vijver R, Van Steenberge, Paul HM, D'hooge DR, Cuoci A, et al. The chemistry of chemical recycling of solid plastic waste via pyrolysis and gasification: state-of-the-art, challenges, and future directions. Prog Energy Combust Sci 2021;84:100901. https://doi.org/10.1016/j.pecs.2020.100901.
[15] Butler E, Devlin G, McDonnell K. Waste polyolefins to liquid fuels via pyrolysis: review of commercial state-of-the-art and recent laboratory research. Waste Biomass Valorization 2011;2:227–55. https://doi.org/10.1007/s12649-011-9067-5.
[16] Wong SL, Ngadi N, Abdullah TAT, Inuwa IM. Current state and future prospects of plastic waste as source of fuel: a review. Renewable Sustainable Energy Rev 2015;50:1167–80. https://doi.org/10.1016/j.rser.2015.04.063.
[17] Dai L, Zhou N, Lv Y, Cheng Y, Wang Y, Liu Y, et al. Pyrolysis technology for plastic waste recycling: a state-of-the-art review. Prog Energy Combust Sci 2022;93:101021. https://doi.org/10.1016/j.pecs.2022.101021.
[18] Palos R, Gutiérrez A, Vela FJ, Olazar M, Arandes JM, Bilbao J. Waste refinery: the valorization of waste plastics and end-of-life tires in refinery units. A review. Energy Fuel 2021;35:3529–57. https://doi.org/10.1021/acs.energyfuels.0c03918.
[19] Huang J, Veksha A, Chan WP, Giannis A, Lisak G. Chemical recycling of plastic waste for sustainable material management: a prospective review on catalysts and processes. Renewable Sustainable Energy Rev 2022;154:111866. https://doi.org/10.1016/j.rser.2021.111866.
[20] Ray R, Thorpe RB. A comparison of gasification with pyrolysis for the recycling of plastic containing wastes. Int J Chem React Eng 2007;5. https://doi.org/10.2202/1542-6580.1504.
[21] Antelava A, Jablonska N, Constantinou A, Manos G, Salaudeen SA, Dutta A, et al. Energy potential of plastic waste valorization: a short comparative assessment of pyrolysis versus gasification. Energy Fuel 2021;35:3558–71. https://doi.org/10.1021/acs.energyfuels.0c04017.
[22] Abbas-Abadi MS, Ureel Y, Eschenbacher A, Vermeire FH, Varghese RJ, Oenema J, et al. Challenges and opportunities of light olefin production via thermal and catalytic pyrolysis of end-of-life polyolefins: towards full recyclability. Prog Energy Combust Sci 2023;96:101046. https://doi.org/10.1016/j.pecs.2022.101046.
[23] Ismail MM, Dincer I. A new renewable energy based integrated gasification system for hydrogen production from plastic wastes. Energy 2023;270:126869. https://doi.org/10.1016/j.energy.2023.126869.
[24] Falascino E, Joshi RK, Kovach L, Isom L, Tong A, Fan L. Biomass chemical looping: advancements and strategies with the moving bed reactor for gasification and hydrogen generation. Energy 2023;285:129326. https://doi.org/10.1016/j.energy.2023.129326.
[25] Lopez G, Artetxe M, Amutio M, Bilbao J, Olazar M. Thermochemical routes for the valorization of waste polyolefinic plastics to produce fuels and chemicals. A review. Renewable Sustainable Energy Rev 2017;73:346–68. https://doi.org/10.1016/j.rser.2017.01.142.
[26] Nanda S, Berruti F. Thermochemical conversion of plastic waste to fuels: a review. Environ Chem Lett 2021;19:123–48. https://doi.org/10.1007/s10311-020-01094-7.
[27] Abbas-Abadi MS, Ureel Y, Eschenbacher A, Vermeire FH, Varghese RJ, Oenema J, et al. Challenges and opportunities of light olefin production via thermal and catalytic pyrolysis of end-of-life polyolefins: towards full recyclability. Prog Energy Combust Sci 2023;96:101046. https://doi.org/10.1016/j.pecs.2022.101046.
[28] Anuar Sharuddin SD, Abnisa F, Wan Daud, Wan Mohd Ashri, Aroua MK. A review on pyrolysis of plastic wastes. Energy Convers Manag 2016;115:308–26. https://doi.org/10.1016/j.enconman.2016.02.037.
[29] Tian X, Zeng Z, Liu Z, Dai L, Xu J, Yang X, et al. Conversion of low-density polyethylene into monocyclic aromatic hydrocarbons by catalytic pyrolysis: comparison of HZSM-5, Hβ, HY and MCM-41. J Clean Prod 2022;358:131989. https://doi.org/10.1016/j.jclepro.2022.131989.
[30] Cortazar M, Santamaria L, Lopez G, Alvarez J, Zhang L, Wang R, et al. A comprehensive review of primary strategies for tar removal in biomass gasification. Energy Convers Manag 2023;276:116496. https://doi.org/10.1016/j.enconman.2022.116496.
[31] Bobadilla LF, Azancot L, González-Castaño M, Ruíz-López E, Pastor-Pérez L, Durán-Olivencia FJ, et al. Biomass gasification, catalytic technologies and energy integration for production of circular methanol: new horizons for industry decarbonisation. J Environ Sci 2024;140:306–18. https://doi.org/10.1016/j.jes.2023.09.020.
[32] Alves CT, Onwudili JA, Ghorbannezhad P, Kumagai S. A review of the thermochemistries of biomass gasification and utilisation of gas products. R Soc Chem 2023;7:3505–40. https://doi.org/10.1039/D3SE00365E.
[33] Jeong Y, Kim J, Ra HW, Seo MW, Mun T, Kim J. Characteristics of air gasification of 10 different types of plastic in a two-stage gasification process. ACS Sustainable Chem Eng 2022;10:4705–16. https://doi.org/10.1021/acssuschemeng.2c00251.
[34] Choi Y, Wang S, Yoon YM, Jang JJ, Kim D, Ryu H, et al. Sustainable strategy for converting plastic waste into energy over pyrolysis: a comparative study of fluidized-bed and fixed-bed reactors. Energy 2024;286:129564. https://doi.org/10.1016/j.energy.2023.129564.
[35] Nugroho RAA, Alhikami AF, Wang W. Thermal decomposition of polypropylene plastics through vacuum pyrolysis. Energy 2023;277:127707. https://doi.org/10.1016/j.energy.2023.127707.
[36] Santamaria L, Lopez G, Fernandez E, Cortazar M, Arregi A, Olazar M, et al. Progress on catalyst development for the steam reforming of biomass and waste plastics pyrolysis volatiles: a review. Energy Fuel 2021;35:17051–84. https://doi.org/10.1021/acs.energyfuels.1c01666.
[37] Lopez G, Artetxe M, Amutio M, Alvarez J, Bilbao J, Olazar M. Recent advances in the gasification of waste plastics. A critical overview. Renewable Sustainable Energy Rev 2018;82:576–96. https://doi.org/10.1016/j.rser.2017.09.032.
[38] Williams PT. Hydrogen and carbon nanotubes from pyrolysis-catalysis of waste plastics: a review. Waste Biomass Valorization 2021;12:1–28. https://doi.org/10.1007/s12649-020-01054-w.
[39] Wu C, Williams PT. Pyrolysis-gasification of plastics, mixed plastics and real-world plastic waste with and without Ni-Mg-Al catalyst. Fuel 2010;89:3022–32. https://doi.org/10.1016/j.fuel.2010.05.032.
[40] Al-asadi M, Miskolczi N, Eller Z. Pyrolysis-gasification of wastes plastics for syngas production using metal modified zeolite catalysts under different ratio of nitrogen/oxygen. J Clean Prod 2020;271:122186. https://doi.org/10.1016/j.jclepro.2020.122186.

[41] Chai Y, Gao N, Wang M, Wu C. H_2 production from co-pyrolysis/gasification of waste plastics and biomass under novel catalyst Ni-CaO-C. Chem Eng J 2020;382:122947. https://doi.org/10.1016/j.cej.2019.122947.

[42] Farooq A, Moogi S, Jang S, Kannapu HPR, Valizadeh S, Ahmed A, et al. Linear low-density polyethylene gasification over highly active Ni/CeO_2-ZrO_2 catalyst for enhanced hydrogen generation. J Ind Eng Chem 2021;94:336–42. https://doi.org/10.1016/j.jiec.2020.11.005.

[43] Yao D, Li H, Dai Y, Wang C. Impact of temperature on the activity of Fe-Ni catalysts for pyrolysis and decomposition processing of plastic waste. Chem Eng J 2021;408:127268. https://doi.org/10.1016/j.cej.2020.127268.

[44] Jiang Y, Li X, Li C, Zhang L, Zhang S, Li B, et al. Pyrolysis of typical plastics and coupled with steam reforming of their derived volatiles for simultaneous production of hydrogen-rich gases and heavy organics. Renew Energy 2022;200:476–91. https://doi.org/10.1016/j.renene.2022.09.120.

[45] Kumagai S, Yabuki R, Kameda T, Saito Y, Yoshioka T. Impact of Ni/Mg/Al catalyst composition on simultaneous H_2-rich syngas recovery and toxic HCN removal through a two-step polyurethane pyrolysis and steam reforming process. Ind Eng Chem Res 2020;59:9023–33. https://doi.org/10.1021/acs.iecr.0c00931.

[46] Kumagai S, Hosaka T, Kameda T, Yoshioka T. Removal of toxic HCN and recovery of H_2-rich syngas via catalytic reforming of product gas from gasification of polyimide over Ni/Mg/Al catalysts. J Anal Appl Pyrolysis 2017;123:330–9. https://doi.org/10.1016/j.jaap.2016.11.012.

[47] Park Y, Namioka T, Sakamoto S, Min T, Roh S, Yoshikawa K. Optimum operating conditions for a two-stage gasification process fueled by polypropylene by means of continuous reactor over ruthenium catalyst. Fuel Process Technol 2010;91:951–7. https://doi.org/10.1016/j.fuproc.2009.10.014.

[48] Czernik S, French RJ. Production of hydrogen from plastics by pyrolysis and catalytic steam reform. Energy Fuel 2006;20:754–8. https://doi.org/10.1021/ef050354h.

[49] Barbarias I, Lopez G, Artetxe M, Arregi A, Bilbao J, Olazar M. Valorisation of different waste plastics by pyrolysis and in-line catalytic steam reforming for hydrogen production. Energy Convers Manag 2018;156:575–84. https://doi.org/10.1016/j.enconman.2017.11.048.

[50] Kim J, Jeong Y, Kim J, Kim J. Two-stage thermochemical conversion of polyethylene terephthalate using steam to produce a clean and H_2- and CO-rich syngas. Energy 2023;276:127651. https://doi.org/10.1016/j.energy.2023.127651.

[51] Arregi A, Amutio M, Lopez G, Bilbao J, Olazar M. Evaluation of thermochemical routes for hydrogen production from biomass: a review. Energy Convers Manag 2018;165:696–719. https://doi.org/10.1016/j.enconman.2018.03.089.

[52] Barbarias I, Artetxe M, Lopez G, Arregi A, Bilbao J, Olazar M. Influence of the conditions for reforming HDPE pyrolysis volatiles on the catalyst deactivation by coke. Fuel Process Technol 2018;171:100–9. https://doi.org/10.1016/j.fuproc.2017.11.003.

[53] Aminu I, Nahil MA, Williams PT. Hydrogen from waste plastics by two-stage pyrolysis/low-temperature plasma catalytic processing. Energy Fuel 2020;34:11679–89. https://doi.org/10.1021/acs.energyfuels.0c02043.

[54] Czernik S, French R. Distributed production of hydrogen by auto-thermal reforming of fast pyrolysis bio-oil. Int J Hydrogen Energy 2014;39:744–50. https://doi.org/10.1016/j.ijhydene.2013.10.134.

[55] Cai W, Wang F, Zhan E, Van Veen AC, Mirodatos C, Shen W. Hydrogen production from ethanol over Ir/CeO_2 catalysts: a comparative study of steam reforming, partial oxidation and oxidative steam reforming. J Catal 2008;257:96–107. https://doi.org/10.1016/j.jcat.2008.04.009.

[56] Cui X, Kær SK. Thermodynamic analysis of steam reforming and oxidative steam reforming of propane and butane for hydrogen production. Int J Hydrogen Energy 2018;43:13009–21. https://doi.org/10.1016/j.ijhydene.2018.05.083.

[57] Lopez G, Garcia I, Arregi A, Santamaria L, Amutio M, Artetxe M, et al. Thermodynamic assessment of the oxidative steam reforming of biomass fast pyrolysis volatiles. Energy Convers Manag 2020;214:112889. https://doi.org/10.1016/j.enconman.2020.112889.

[58] Barbarias I, Lopez G, Alvarez J, Artetxe M, Arregi A, Bilbao J, et al. A sequential process for hydrogen production based on continuous HDPE fast pyrolysis and in-line steam reforming. Chem Eng J 2016;296:191–8. https://doi.org/10.1016/j.cej.2016.03.091.

[59] Fernandez E, Santamaria L, Artetxe M, Amutio M, Arregi A, Lopez G, et al. Conditioning the volatile stream from biomass fast pyrolysis for the attenuation of steam reforming catalyst deactivation. Fuel 2022;312:122910. https://doi.org/10.1016/j.fuel.2021.122910.

[60] Barbarias I, Artetxe M, Lopez G, Arregi A, Santamaria L, Bilbao J, et al. Catalyst performance in the HDPE pyrolysis-reforming under reaction-regeneration cycles. Catalyst 2019;9:414. https://doi.org/10.3390/catal9050414.

[61] Erkiaga A, Lopez G, Barbarias I, Artetxe M, Amutio M, Bilbao J, et al. HDPE pyrolysis-steam reforming in a tandem spouted bed-fixed bed reactor for H2 production. J Anal Appl Pyrolysis 2015;116:34–41. https://doi.org/10.1016/j.jaap.2015.10.010.

[62] Lopez G, Erkiaga A, Artetxe M, Amutio M, Bilbao J, Olazar M. Hydrogen production by high density polyethylene steam gasification and in-line volatile reforming. Ind Eng Chem Res 2015;54:9536–44. https://doi.org/10.1021/acs.iecr.5b02413.

[63] Barbarias I, Lopez G, Artetxe M, Arregi A, Santamaria L, Bilbao J, et al. Pyrolysis and in-line catalytic steam reforming of polystyrene through a two-step reaction system. J Anal Appl Pyrolysis 2016;122:502–10. https://doi.org/10.1016/j.jaap.2016.10.006.

[64] Arregi A, Seifali Abbas-Abadi M, Lopez G, Santamaria L, Artetxe M, Bilbao J, et al. CeO_2 and La_2O_3 promoters in the steam reforming of polyolefinic waste plastic pyrolysis volatiles on Ni-based catalysts. ACS Sustainable Chem Eng 2020;8:17307–21. https://doi.org/10.1021/acssuschemeng.0c06800.

[65] Elordi G, Olazar M, Lopez G, Artetxe M, Bilbao J. Product yields and compositions in the continuous pyrolysis of high-density polyethylene in a conical spouted bed reactor. Ind Eng Chem Res 2011;50:6650–9. https://doi.org/10.1021/ie200186m.

[66] Barbarias I, Lopez G, Amutio M, Artetxe M, Alvarez J, Arregi A, et al. Steam reforming of plastic pyrolysis model hydrocarbons and catalyst deactivation. Appl Catal, A 2016;527:152–60. https://doi.org/10.1016/j.apcata.2016.09.003.

[67] Altzibar H, Lopez G, Bilbao J, Olazar M. Minimum spouting velocity of conical spouted beds equipped with draft tubes of different configuration. Ind Eng Chem Res 2013;52:2995–3006. https://doi.org/10.1021/ie302407f.

[68] Makibar J, Fernandez-Akarregi AR, Díaz L, Lopez G, Olazar M. Pilot scale conical spouted bed pyrolysis reactor: draft tube selection and hydrodynamic performance. Powder Technol 2012;219:49–58. https://doi.org/10.1016/j.powtec.2011.12.008.

[69] Nagashima H, Ishikura T, Ide M. Effect of the tube shape on gas and particle flow in spouted beds with a porous draft tube. Can J Chem Eng 2009;87:228–36. https://doi.org/10.1002/cjce.20150.

[70] Neto JLV, Duarte CR, Murata VV, Barrozo MAS. Effect of a draft tube on the fluid dynamics of a spouted bed: experimental and CFD studies. Dry Technol 2008;26:299–307. https://doi.org/10.1080/07373930801897994.

[71] Mollick PK, Pandit AB, Vijayan PK. Parameters affecting efficient solid circulation rate in draft tube spouted bed. Ind Eng Chem Res 2018;57:8605–11. https://doi.org/10.1021/acs.iecr.8b01691.

[72] Cortazar M, Lopez G, Alvarez J, Amutio M, Bilbao J, Olazar M. Advantages of confining the fountain in a conical spouted bed reactor for biomass steam gasification. Energy 2018;153:455–63. https://doi.org/10.1016/j.energy.2018.04.067.

[73] Tsuji T, Hatayama A. Gasification of waste plastics by steam reforming in a fluidized bed. J Mater Cycles Waste Manage 2009;11:144–7. https://doi.org/10.1007/s10163-008-0227-z.

[74] Cortazar M, Alvarez J, Lopez G, Amutio M, Santamaria L, Bilbao J, et al. Role of temperature on gasification performance and tar composition in a fountain enhanced conical spouted bed reactor. Energy Convers Manag 2018;171:1589–97. https://doi.org/10.1016/j.enconman.2018.06.071.

[75] Cortazar M, Gao N, Quan C, Suarez MA, Lopez G, Orozco S, et al. Analysis of hydrogen production potential from waste plastics by pyrolysis and in line oxidative steam reforming. Fuel Process Technol 2022;225:107044. https://doi.org/10.1016/j.fuproc.2021.107044.

[76] Kang I, Bae J. Autothermal reforming study of diesel for fuel cell application. J Power Sources 2006;159:1283–90. https://doi.org/10.1016/j.jpowsour.2005.12.048.

[77] Kang I, Bae J, Bae G. Performance comparison of autothermal reforming for liquid hydrocarbons, gasoline and diesel for fuel cell applications. J Power Sources 2006;163:538–46. https://doi.org/10.1016/j.jpowsour.2006.09.035.

[78] Palm C, Cremer P, Peters R, Stolten D. Small-scale testing of a precious metal catalyst in the autothermal reforming of various hydrocarbon feeds. J Power Sources 2002;106:231–7. https://doi.org/10.1016/S0378-7753(01)01018-7.

[79] Navarro Yerga RM, Álvarez-Galván MC, Mota N, VilloriadelaMano JA, Al-Zahrani S, Fierro JLG. Catalysts for hydrogen production from heavy hydrocarbons. ChemCatChem 2011;3:440–57. https://doi.org/10.1002/cctc.201000315.

[80] Alvarez-Galvan MC, Navarro RM, Rosa F, Briceño Y, Ridao MA, Fierro JLG. Hydrogen production for fuel cell by oxidative reforming of diesel surrogate: influence of ceria and/or lanthana over the activity of Pt/Al_2O_3 catalysts. Fuel 2008;87:2502–11. https://doi.org/10.1016/j.fuel.2008.03.003.

[81] Czernik S, French RJ. Production of hydrogen from plastics by pyrolysis and catalytic steam reform. Energy Fuel 2006;20:754–8. https://doi.org/10.1021/ef050354h.

[82] Namioka T, Saito A, Inoue Y, Park Y, Min T, Roh S, et al. Hydrogen-rich gas production from waste plastics by pyrolysis and low-temperature steam reforming over a ruthenium catalyst. Appl Energy 2011;88:2019–26. https://doi.org/10.1016/j.apenergy.2010.12.053.

[83] Wu C, Williams PT. Effects of gasification temperature and catalyst ratio on hydrogen production from catalytic steam pyrolysis-gasification of polypropylene. Energy Fuel 2008;22:4125–32. https://doi.org/10.1021/ef800574w.

[84] Wu C, Williams PT. Hydrogen production from the pyrolysis-gasification of polypropylene: influence of steam flow rate, carrier gas flow rate and gasification temperature. Energy Fuel 2009;23:5055–61. https://doi.org/10.1021/ef900278w.

[85] Al-asadi M, Miskolczi N. Hydrogen rich products from waste HDPE/LDPE/PP/PET over Me/Ni-ZSM-5 catalysts combined with dolomite. J Energy Inst 2021;96:251–9. https://doi.org/10.1016/j.joei.2021.03.004.

[86] Khan MFA, Khan A, Ibrahim H, Idem R. Kinetic study of the catalytic partial oxidation of synthetic diesel over 5 wt% Ni/$Ce_{0.5}Zr_{0.33}Ca_{0.085}Y_{0.085}O_{2-\delta}$ catalyst for hydrogen production. Energy Fuel 2012;26:5421–9. https://doi.org/10.1021/ef301075y.

[87] Erkiaga A, Lopez G, Amutio M, Bilbao J, Olazar M. Syngas from steam gasification of polyethylene in a conical spouted bed reactor. Fuel 2013;109:461–9. https://doi.org/10.1016/j.fuel.2013.03.022.

[88] Wilk V, Hofbauer H. Conversion of mixed plastic wastes in a dual fluidized bed steam gasifier. Fuel 2013;107:787–99. https://doi.org/10.1016/j.fuel.2013.01.068.

[89] He M, Xiao B, Hu Z, Liu S, Guo X, Luo S. Syngas production from catalytic gasification of waste polyethylene: influence of temperature on gas yield and composition. Int J Hydrogen Energy 2009;34:1342–8. https://doi.org/10.1016/j.ijhydene.2008.12.023.
[90] Shilov VA, Rogozhnikov VN, Potemkin DI, Belyaev VD, Shashkov MV, Sobyanin VA, et al. The influence of aromatic compounds on the Rh-containing structured catalyst performance in steam and autothermal reforming of diesel fuel. Int J Hydrogen Energy 2022;47:11316–25. https://doi.org/10.1016/j.ijhydene.2021.08.226.
[91] Sahu MK, Sinha ASK. Oxidative steam reforming of vacuum residue for hydrogen production. Int J Hydrogen Energy 2012;37:1425–35. https://doi.org/10.1016/j.ijhydene.2011.09.142.
[92] Xu X, Zhang S, Li P. Autothermal reforming of n-dodecane and desulfurized Jet-A fuel for producing hydrogen-rich syngas. Int J Hydrogen Energy 2014;39:19593–602. https://doi.org/10.1016/j.ijhydene.2014.09.124.
[93] Jo SB, Ju DG, Jung SY, Ha DS, Chae HJ, Lee SC, et al. Performance of an auto-reduced nickel catalyst for auto-thermal reforming of dodecane. Catalysts 2018;8:371. https://doi.org/10.3390/catal8090371.
[94] Yao D, Zhang Y, Williams PT, Yang H, Chen H. Co-production of hydrogen and carbon nanotubes from real-world waste plastics: influence of catalyst composition and operational parameters. Appl Catal, B 2018;221:584–97. https://doi.org/10.1016/j.apcatb.2017.09.035.
[95] Wang S, zhang Y, Shan R, Gu J, Huhe T, Ling X, et al. High-yield H_2 production from polypropylene through pyrolysis-catalytic reforming over activated carbon based nickel catalyst. J Clean Prod 2022;352:131566. https://doi.org/10.1016/j.jclepro.2022.131566.
[96] Qi A, Wang S, Fu G, Wu D. Autothermal reforming of n-octane on Ru-based catalysts. Appl Catal, A 2005;293:71–82. https://doi.org/10.1016/j.apcata.2005.07.009.
[97] Wu C, Nahil MA, Miskolczi N, Huang J, Williams PT. Processing real-world waste plastics by pyrolysis-reforming for hydrogen and high-value carbon nanotubes. Environ Sci Technol 2014;48:819–26. https://doi.org/10.1021/es402488b.
[98] Cheekatamarla PK, Lane AM. Catalytic autothermal reforming of diesel fuel for hydrogen generation in fuel cells: I. Activity tests and sulfur poisoning. J Power Sources 2005;152:256–63. https://doi.org/10.1016/j.jpowsour.2005.03.209.
[99] Yao D, Yang H, Chen H, Williams PT. Co-precipitation, impregnation and so-gel preparation of Ni catalysts for pyrolysis-catalytic steam reforming of waste plastics. Appl Catal, B 2018;239:565–77. https://doi.org/10.1016/j.apcatb.2018.07.075.
[100] Zhou H, Saad JM, Li Q, Xu Y. Steam reforming of polystyrene at a low temperature for high H_2/CO gas with bimetallic Ni-Fe/ZrO_2 catalyst. Waste Manage 2020;104:42–50. https://doi.org/10.1016/j.wasman.2020.01.017.
[101] Zhang Y, Huang J, Williams PT. Fe-Ni-MCM-41 catalysts for hydrogen-rich syngas production from waste plastics by pyrolysis-catalytic steam reforming. Energy Fuel 2017;31:8497–504. https://doi.org/10.1021/acs.energyfuels.7b01368.
[102] Nahil MA, Wu C, Williams PT. Influence of metal addition to Ni-based catalysts for the co-production of carbon nanotubes and hydrogen from the thermal processing of waste polypropylene. Fuel Process Technol 2015;130:46–53. https://doi.org/10.1016/j.fuproc.2014.09.022.
[103] Acomb JC, Wu C, Williams PT. Control of steam input to the pyrolysis-gasification of waste plastics for improved production of hydrogen or carbon nanotubes. Appl Catal, B 2014;147:571–84. https://doi.org/10.1016/j.apcatb.2013.09.018.
[104] Hwang I, Kobayashi J, Kawamoto K. Characterization of products obtained from pyrolysis and steam gasification of wood waste, RDF, and RPF. Waste Manage 2014;34:402–10. https://doi.org/10.1016/j.wasman.2013.10.009.